Check for updates

Predicting airborne pollutant concentrations and events in a commercial building using low-cost pollutant sensors and machine learning: A case study

Ahmad Mohammadshirazi, Vahid Ahmadi Kalkhorani, Joseph Humes, Benjamin Speno, Juliette Rike, Rajiv Ramnath, Jordan D. Clark [*]

The Ohio State University, College of Engineering, 221C Bolz Hall, 2036 Neil Avenue, Columbus, OH, 43210, USA

ARTICLE INFO

ABSTRACT

Prediction of indoor airborne pollutant concentrations can enable a smart indoor air quality control strategy that potentially reduces building energy use and improves occupant comfort. In service of this overarching goal, this work pursues four objectives: 1) Determine which low-cost airborne pollutant sensors are useful for prediction of indoor air quality variables of interest, investigating whether a few commercially available sensors held value for making such predictions. 2) Investigate which algorithms are most useful for making these predictions. 3) Develop an understanding of how far into the future we can conceivably predict indoor concentrations based on low-cost airborne pollutant signals. 4) Investigate methods for predicting elevated concentration events from historical data. Four different methods (Rolling Average, Random Forest, Gradient Boosting, and Long-Short Term Memory) for predicting eight indoor pollutant concentrations (carbon dioxide, nitrogen dioxide, ozone, PM 1, PM 2.5, PM 10, formaldehyde, total volatile organic compounds) are compared for their ability to predict future sensor signals in a single commercial building in California. Long-Short Term Memory was consistently the best method for predicting indoor pollutants, though the best combinations of input variables differed depending on pollutant of interest. To predict elevated concentration events, results show that indirect classification through a regression prediction that was then compared to a threshold performed marginally better than a direct classification prediction for all pollutants except PM_1.

1. Introduction

Exposure to airborne indoor pollutants such as mold, radon, secondhand smoke, formaldehyde, and airborne fine particles is correlated to adverse health effects, including asthma and lung cancer [1] among others. To control concentrations of these pollutants and mitigate health effects, commercial buildings are typically provided with a relatively simple combination of particle filtration with prescribed removal effectiveness in central air handling units, source control, and prescriptive quantities of ventilation air supplied to the building while it is occupied [2]. This results in expenditure of few percent of all source energy used in the United States each year [3]. Commercial buildings also contribute between 33% and 45% of summer peak demand [4,5], of which a large fraction is attributable to ventilation, perhaps upwards of 10% of all peak power demand [6].

Moving to a smarter control paradigm using a fully optimized, data-driven approach with ubiquitous sensors offers the possibility of improved indoor environments and more energy efficient delivery of these environments. Smart building systems have offered immense benefits in many areas, with much of the research on smart building systems centering on thermal control. Several reviews of such smart building technologies exist [7,8].

Provision of indoor air quality, despite its well-established link with occupant health, comfort, and productivity, is one of the less-studied smart building functions. However, recently, in an attempt to provide better indoor environments more efficiently, research has commenced on "smart" control of ventilation systems and air cleaning in which one or more continuously measured variables is used as an input to a responsive control ventilation or air cleaning device controller. Early efforts at smart control involved only an accounting of volumetric flow rates of ventilation air and perhaps non-air quality signals such as

---

Abbreviations

MSE	Mean Squared Error
RF	Random Forest
GB	Gradient Boosting
LSTM	Long-Short Term Memory
RTT	Ratio of Testing-Training
_in	Indoor
_out	Outdoor
num_week	Number of day in a week
num_year	Number of day in a year
TP	True Positive
TN	True Negative
FP	False Positive
FN	False Negative

outdoor temperature, occupancy, and relative humidity. A few recent reviews of smart air quality control in residences are available [9,10]. Less et al. (2019) quantified the energy savings of ventilation control strategies in California residences that responded to outdoor temperature signals, as opposed to providing constant airflow. For the most effective strategies, up to 55% of heating costs were saved on average, accounting for 15% of all HVAC costs [11]. Clark et al. (2019) found little improvement in these strategies was available by adding occupancy sensing [12]. Young et al. (2020) found that similar strategies could be used to remove nearly all peak electric power demand due to ventilation in most building types [6]. Less et al. (2020) extended previous work to include multi-zone approaches, which offered marginal benefits [13].

An emerging improvement to these flow-based smart control strategies is the integration of signals from low-cost airborne pollutant sensors, which are being studied heavily for indoor environmental monitoring and control [14–33]. A sampling of commercially available low-cost airborne pollutant sensors and their specifications is given in Appendix A. Low-cost airborne pollutant sensors come in many forms, with perhaps the most common being optical sensors that use the interaction of light with a pollutant to ascertain characteristics about the pollutant. For example, optical particle sensors detect particles by seeing how a light source is scattered by the particulate matter in the air [34]. Other kinds of sensors include electrochemical, solid-state, catalytic, photo-ionization, non-dispersive infrared, and metal oxide sensors [35].

The performance of these sensors under laboratory and field conditions has been studied extensively, especially for low-cost particle sensors [14–34,36–54] and continues to improve rapidly, although they are still known to suffer from several classes of errors, which has prevented their wide-scale uptake in the industry to date. These errors include non-linearity [55], signal drift [56], cross-substance sensitivity, variations in performance with environmental conditions, different performance when measuring different concentrations and other variations in conditions [57]. However, some of the best sensors (especially particle sensors) have been shown to give performance similar to much more expensive instruments [44]. Also, it should be noted that in some applications, the absolute accuracy of a sensor is less important for making control decisions than is the sensor signal relative to a baseline (e.g. activating a filtration system during an indoor particle emission event) and therefore "inaccurate" sensor signals may still be of value. There is also evidence in the literature that inaccurate sensor signals can be made more accurate through post-processing of sensor signals in software [34].

Low-cost fine particle sensors for potential application in indoor environments have been tested more extensively and with better results than low-cost gas sensors in the literature [93–102,105,106,109,111], owing to the fact that the low-cost particle sensing technology (almost always optical sensing with inexpensive LEDs) is considered more mature and robust that low-cost gas sensing technology. Testing of gas sensors for indoor air quality monitoring has been published, however, with mixed results [58,59]. Another challenge in gas sensing is the multitude of gases of interest and the specificity needed in a sensor to give useful information. Formaldehyde is perhaps the most important gase in indoor environments for chronic health concerns [60] and real-time monitoring of formaldehyde with even ~$1–2000 devices is still in need of improvement as evidenced by the few field studies on the subject, e.g. Ref. [61]. Nonetheless, as explained above, less-than-accurate sensors may offer some utility for registering high-concentration events. For this reason, we did explore the use of low-cost gas sensors in this work to predict high concentration events and expect commercially available gas sensors to have some utility for this application.

In addition to the signals from the sensors themselves, software post-processing of low-cost pollutant signals can provide additional valuable information. Post-processing can range from simple linear corrections for environmental conditions, to fully optimized predictive control algorithms using a multitude of sensor signals and other information. The latter has been explored very little in the literature and motivates the current work. Chen et al. (2018) predicted time series of three gases in an academic building using machine learning using measurements from higher-cost reference grade instruments, with support vector machine algorithms providing the best predictions [54]. They were able to predict carbon dioxide (CO_2) and total volatile organic compounds with relative success, but were unable to predict formaldehyde concentrations. Ahn et al. (2017) applied Long Short-Term Memory (LSTM) and gated recurrent units models to predict environmental variables including dust concentration in an indoor environment [57]. Zhang et al. (2021) used artificial neural networks to predict emissions of VOCs from furniture [62]. Algorithms used in other applications likely hold some promise for predicting and controlling air quality in buildings in a data-driven way [57]. Recently, Tang et al. [63] used the Random Forest model to predict fine particle emission events in 18 apartments and 65 new homes with a high degree of success.

Machine learning and deep learning models have been employed successfully in other sub-disciplines within building science, including building thermal load prediction [64], commercial building energy consumption prediction, and other disciplines [65–71]. We expect similar advances are possible when machine learning is applied to indoor air quality prediction as well.

1.1. Scope and objectives

In this work, we attempted to apply machine learning algorithms popular in other applications to prediction of air quality in a commercial building to gain insights on paths forward for data-driven air quality control in buildings.

Our objectives are to (1) determine which algorithms are most useful for making these predictions, (2) determine which low-cost pollutant sensors are useful for prediction of indoor air quality variables in the building studied, including making a determination as to whether a few commercially available sensors held value for making such predictions, (3) develop an understanding of how far into the future we can conceivably predict indoor concentrations based on low-cost airborne pollutant signals, and (4) develop methods for predicting elevated concentration events from historical data.

This work is not concerned with establishing the "ground truth" for comparison of low-cost sensor outputs with those of more sophisticated measurement techniques, but rather with the prediction of sensor signals based on previous outputs of these same sensors. We leave it to others to establish the accuracy of each sensor, and much of this work is being done or has been done. The scope of this work is also not concerned with control, but rather with prediction of time series of pollutant concentrations given historical concentrations, and with prediction of

elevated concentration events.

2. Methodology

We first describe the data used in the investigation, and then the methods for analysis and prediction, and finally the metrics used to evaluate the performance of the methods tested.

2.1. Data

2.1.1. Indoor data

We analyzed data from a set of sensors located inside a single mixed use building in California. The building is primarily office space and conference rooms but contains small dry labs as well. Researchers at the Lawrence Berkeley National Laboratory collected readings for eight indoor airborne pollutants every minute, including carbon dioxide (CO_2), nitrogen dioxide (NO_2), ozone (O_3), particulate matter of three different nominal sizes (PM_1, $PM_{2.5}$, and PM_{10}), a signal referred to as TVOCs, and formaldehyde (HCHO), as well as the indoor temperature (T), relative humidity (RH), and pressure (P) from October 25, 2019 to March 14, 2020, dates inclusive. This data was recorded using low-cost sensors, which were dispersed throughout the interior of a five story building located in Berkeley, California. Suites of these eight sensors were located in various parts of the building, including offices, entryways, conference rooms, hallways, lounges, and a single suite located on the roof. The specifications of each sensor are given in Table 1. All specifications are manufacturer-reported unless otherwise noted.

All sensors were located in common areas such as hallways, entryways and conference rooms and exposed to the public. A typical example of sensor placement is provided in Fig. 1 as shown below:

Because the time resolution of the indoor sensors varied, we averaged our data to an hourly resolution to match the hourly resolution of the outdoor data described below. This allowed us to provide consistent inputs to our prediction algorithms. Further, previous work has suggested that at time scales less than 1 h, sensor noise and other factors cause accuracy of low-cost sensor signals to rapidly decrease [43]; hence we believe that averaging made our data more accurate as well.

2.1.2. Outdoor data

In addition to indoor sensor data, we used outdoor data as inputs to our predictive algorithms, anticipating the effect of outdoor conditions on concentrations of indoor pollutants. We used outdoor concentration data for CO_2, NO_2, O_3, PM_1, $PM_{2.5}$ and PM_{10}, along with T and RH data. We pulled this data from public datasets available from three websites [72–74]:

- CO_2 data was taken from the Berkeley Environmental Air-quality & CO2 Network (BEACO2N) [72]. The website for this network (http://beacon.berkeley.edu/metadata/) lays out various quality control procedures, etc. The nearest monitoring station to the project site was 0.39 miles away.
- The PM [74] and RH [74] data were taken from the PurpleAir Network (https://www2.purpleair.com/) [74]. PurpleAir sensors

Fig. 1. A typical example of sensor placement.

have been tested extensively in the literature including [43–45,75, 76] and shown to be among the better of the commercially available low-cost particle sensors along several dimensions. The nearest monitoring site was 0.73 miles from the project site.

- O_3 and NO_2 data were taken from airnowtech.org [73]. The nearest monitoring station is 0.39 miles from the project site.
- The output frequency of all outdoor pollutants is hourly.

While indoor air quality data from sensors was essentially complete, outdoor air measurements had numerous missing data points, as shown in Table B1 in Appendix B. The amount of missing data also varied by pollutant. Thus, for particulate matter (PM_1, $PM_{2.5}$, PM_{10}), relative humidity (RH), and temperature (T), only five or six records (less than one percent) of the data were absent. For these pollutants, we simply filled in the previous datapoint for each missing record. Data from CO_2, NO_2, and O_3 sensors had between 5 and 8% of their original data missing, so more complex methods described in Appendix B were used to interpolate the data.

2.1.3. Other data

Additionally, we included an integer value for time of day and another integer for day of the week as inputs to the prediction algorithms (e.g. data collected on Monday had an additional input of "1" for day of the week, Tuesday gives "2", etc.), as well as a numerical value representing the day of the year ("1" through "365").

2.1.3.1. Input data used for each method.
Since it was not feasible to test all 22 input variables at once, and to reduce the complexity and training time of our models, the list of input variables was down-selected in two phases. First, the list of inputs for predicting each concentration of interest was shortened by considering the contributing factors of each pollutant (i.e. the physics of each pollutant). Thus, we eliminated occupant-related variables such as indoor CO_2 concentration as inputs for pollutants, such as ozone, expected to be primarily generated outdoors. Conversely, we eliminated outdoor pollutant concentrations as inputs for predicting indoor-generated pollutants such as formaldehyde. Combustion bi-products such as NO_2 and particulate matter were retained as inputs for other combustion bi-products, and occupant-

Table 1
Specifications of each pollutant sensor.

Specification	O_3	NO_2	CO_2	PM	HCHO	TVOC
Sensor	Spec 3SP_O3_20 P	Spec 3SP_NO2_5F P	Elichens Foxberry	Plantower PMS 7003	ZE07-CH2O	CCS811-ams
Functional Principle	Electro-chemical	Electro-chemical	nondispersive infrared	optical	Electro-chemical	Electro-chemical
Range	20 ppb - 20 ppm	20 ppb - 20 ppm	0–10000 ppm	0–500 µg/m^3	0–5 ppm	0ppb–32768 ppb
Reproducibility	±10 ppb ±5%	±10 ppb ±5%		±10µg/m3 ± 10%		
Sensitivity	−60 ± 10 nA/ppm	−60 ± 10 nA/ppm				
Cross Sensitivity	NO2	O3[a]				
Accuracy			±30 ppm ±2%		0.01 ppm	±2%
Reference	[77]	[78]	[79]	[80]	[81]	[82]

[a] Includes a filter for the labeled pollutant.

related pollutants such as CO_2 and TVOCs (assumed to be at least in part generated from occupant activities) were retained for prediction of other occupant-related pollutant concentrations. Table 2 shows the inputs used for each predicted concentration listed in the top row after the first down-selection phase.

After this initial down-selection phase, we sought to further reduce the list of input variables needed for prediction of each pollutant concentration. This was done primarily to investigate which sensors were most beneficial in predicting the concentration of another correlated pollutant, in order to help answer the practical question of which minimal suite of sensors should ultimately be installed. We determined which sensor signals were most beneficial for predicting each pollutant of interest by programmatically running all combinations of each potential input variable for each predicted concentration. For example, for PM10 predictions, we tried 2^{11}-1 combinations of 11 potential inputs. For each of these runs we predicted the times series of PM10 concentrations using the methods described in Section 2.2. We did this for four different ratios of training and testing data ("ratio of testing to training" or RTT). We repeated this five times for each RTT to eliminate statistical bias. Thus, for example, for PM_{10} predictions we did $4x5x(2^{11}-1)$ runs to determine the best input variables. Of all the runs, we then looked at the 100 best predictions (based on our evaluation metrics - also discussed in Section 2.3) and counted the number of times each input was present in these 100 best combinations. The number of times the input was present determined the value of that input to the prediction (we report this in the section on Results).

2.2. Methods for prediction

Our primary goals were (a) predict time series of future pollutant concentrations from models built on past concentrations, and (b) predict of high-concentration events. We now describe the methods used for each.

2.2.1. Predicting the time series of future concentrations

From the fully interpolated dataset, we first attempted to predict time series concentrations of eight indoor pollutants: CO_2, NO_2, O_3, and PM_1, $PM_{2.5}$, PM_{10}, HCHO, and "TVOC". We applied four methods: rolling average [83], Random Forest (RF) [84,85], Gradient Boosting (GB) [86, 87], and LSTM models [88–90]. The rolling average method, which takes the average of a number of previous data points to compute the next (future) datapoint, was considered the baseline. We used seven previous data points as our look-back.

RF is a supervised machine learning algorithm frequently used for classification, regression, and other tasks. This method generates a large number of individual uncorrelated decision trees at training time. Then, for classification, each decision tree outputs the class that is the mode of all the individual classes. For regression, each decision tree outputs the

mean (i.e. the average) value generated by each individual tree. Bootstrap aggregating, or bagging, is applied during tree learning during training. This typically leads to a better model due to the decrease of its variance. By ensuring that trees are uncorrelated, they become more robust to noise in the training set [84]. We used 320 estimators when generating the trees. Finally our RF scripts were executed using resources from Google Collab (https://colab.research.google.com/), taking a total of 6 h to complete training and testing.

Like RF, GB is a supervised machine learning technique for regression and classification that relies on the use of decision trees. Base trees of the same size are added iteratively, while existing trees within the model are not changed. GB seeks to minimize the loss when new trees are added to the model [86]. For our work, we used 100 estimators when using this method. Using one GPU node on Google Collab, it took about 7 h to complete training and testing.

The last method discussed is LSTM. LSTM is a modification of recurrent neural networks (RNN) that addresses the RNN shortcoming of loss of earlier information in long temporal records during training. LSTM address this issue by transferring important information from the past while eliminating unnecessary information using a "forget" neural gate [89,90]. LSTM is capable of learning long-term dependencies and is designed to overcome both errors in back-propagation and efficiency issues found in previous short-term memory algorithms. LSTM makes use of memory cells containing input gates and output gates, which control the error flow from both a cell's inputs and outputs by deciding when to override, keep, or access information in a memory cell. An LSTM network contains one input layer, one hidden layer (containing the cells and the gates), and one output layer. Comparisons to traditional short-term memory algorithms have shown that LSTM learns much faster and is more efficient, making it a common tool for modeling sequential data, especially multivariate sequential data [88,89]. We trained our LSTM models for 1000 epochs, using a batch size of 256, a validation split of 10%, and a sub signal size of seven. The activation function used was the Sigmoid function. Architectures of the LSTM models varied by their application (and are discussed with each application). LSTM requires more computational resources. Hence, the LSTM scripts were executed on 62 CPU nodes, each with 40 cores, on the Ohio Supercomputer Center (OSC), taking 19 h to complete training and testing.

Note also that each of our methods used the input data differently. RF and GB looked at a single prior data point, whereas the rolling average looked at seven previous data points and the LSTM method looked at twelve prior data points. Similarly, the output data was also generated differently by the different methods. The Rolling Average, RF, and GB methods generated one data point at a time, while the LSTM method generated batches of consecutive data points.

Table 2
Inputs used for each predicted variable after first down-selection phase (based on physical reasoning).

Indoor concentration predicted for next hour	CO_2	NO_2	O_3	PM_1	$PM_{2.5}$	PM_{10}	CH_2O	TVOC
Current hour input variables used	Hour	Hour	Hour	Hour	Hour	Hour	Hour	Hour
	CO_2_in	NO_2_in	O_3_in	NO_2_in	CO_2_in	CO_2_in	CO_2_in	CO_2_in
	RH_in	T_in	T_in	PM_1_in	$PM_{2.5}$_in	PM_{10}_in	CH_2O_in	TVOC_in
	T_in	NO_2_out	O_3_out	T_in	T_in	T_in	RH_in	RH_in
	CO_2_out	RH_out	RH_out	PM_1_out	$PM_{2.5}$_out	PM_{10}_out	T_in	T_in
	T_out	T_out	T_out	T_out	T_out	T_out	T_out	T_out
	num_week	num_week	num_year	num_year	num_week	num_week	num_week	num_week
	CH_2O_in	CO_2_out	num_week	num_week	NO_2_in	PM_1_in	TVOC_in	CH_2O_in
	TVOC_in	O_3_out	CO_2_out	O_3_in	O_3_in	$PM_{2.5}$_in		
		PM_1_out	NO_2_out	$PM_{2.5}$_in	PM_1_in	PM_1_out		
		$PM_{2.5}$_out	PM_1_out	PM_{10}_in	PM_{10}_in	$PM_{2.5}$_out		
			$PM_{2.5}$_out	NO_2_out	NO_2_out			
				O_3_out	O_3_out			
				$PM_{2.5}$_out	PM_1_out			
				PM_{10}_out	PM_{10}_out			

2.2.2. Predicting high concentration events

In addition to predicting the future time series of concentrations, we also attempted to predict the occurrence of high-concentration events, as a potentially practical method for knowing when to pre-emptively activate a pollutant mitigation device in a building. Several such events were visibly evident in the datasets, likely resulting from an indoor emission event, the introduction of outdoor pollutants, or a combination thereof. Fig. 2 shows an example of 48 h of NO_2 concentrations with clearly evident high-concentration events (the 11 readings circled qualified as high-concentration events - we defined high-concentration events as those whose readings are greater than two standard deviations the average of the readings).

We developed and evaluated two methods for predicting high-concentration events: indirect event classification and direct event classification. For both methods, 20% of the data was held out of training to be used as a test set. We describe the two methods next.

2.2.2.1. Indirect classification.
Here, we first predict whether a high concentration event would occur by predicting a times series of each concentration and then classify each predicted point as an event or a non-event (to repeat, we consider a data point as part of a high-concentration event if its value exceeds the threshold of 2 standard deviations above the mean. The number of events, and the percentage of the data that contains such events in both the training and testing sets (20% RTT) are listed in Table 3.

2.2.2.2. Creating a direct classification model.
Alternatively, events could be predicted directly using classification. In this method, the same inputs were used to predict whether the *next* event (occurring 1 h later) is a high-concentration event. For many practical applications this classification will be sufficient, since an hour's notice is usually sufficient to activate a control device such as an exhaust fan. We used multiple classification methods, including RF, GB, and LSTM. Each of these models used the same architecture and the same RTT of 20% as the corresponding models used for indirect prediction.

2.3. Evaluation metrics

Mean Square Error (MSE) was used as the evaluation metric to find the optimal combination of inputs. The Adjusted R-Squared (Adjusted R^2) is also reported as a secondary metric (adjusted R^2 is not used during training because it is redundant), one that measures the extent of the correlation (i.e. fit) between the predicted and actual values ("fit" is not something MSE can validate, because it is a magnitude). Note also that the R^2 measure has both a standard form and adjusted form. The adjusted R^2 measure accounts for independent variables in the computation of the correlation, providing better insight into the correlations. For our LSTM models, five repetitions were performed for each input
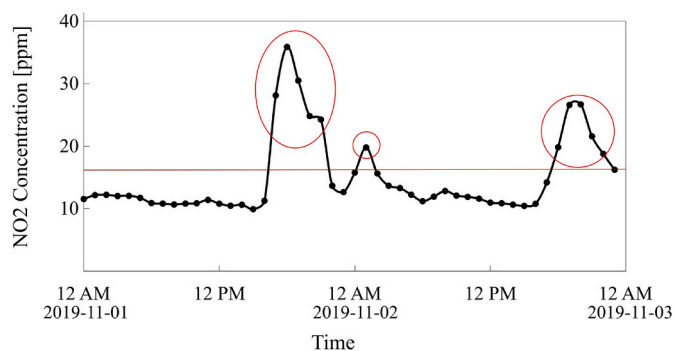

Fig. 2. Time series of NO_2 concentrations over two days with high-concentration events circled. The line at approximately 16 ppm shows the average + 2 standard deviations of the entire dataset.

Table 3
Number of events and the percentage of datapoints classified as high-concentration events for each indoor pollutant over the training and testing datasets.

Pollutant	Number of events Training/(Testing)	Percentage Training/(Testing)
CO_2_in	183/**(24)**	6.78%/**(4.00%)**
NO_2_in	143/**(34)**	5.30%/**(5.67%)**
O_3_in	66/**(70)**	2.44%/**(11.67%)**
PM_1_in	218/**(13)**	8.07%/**(2.17%)**
$PM_{2.5}$_in	197/**(10)**	7.30%/**(1.67%)**
PM_{10}_in	190/**(9)**	7.04%/**(1.50%)**
CH_2O_in	71/**(52)**	2.63%/**(8.67%)**
TVOC_in	80/**(102)**	2.97%/**(17.00%)**

combination to account for random statistical bias. We used RTTs of 5%, 10%, 15%, and 20%. The best values for training and test MSE and Adjusted R^2 are shown in the Results section.

Several different metrics could have been used to evaluate the performance of our models. One of them, accuracy, is the typical metric for such models, and simply looks at the percentage of correct classifications out of the total set of attempts, and includes both true positives and true negatives [91]. However, for datasets such as this one where the number of true positives is vastly outweighed by the number of true negatives, using accuracy as the primary metric can lead to an incorrect perception of performance. Other metrics must be used to evaluate how well a classifier can identify rarer classes. Precision and recall are the most common of these metrics. Precision looks at how many positive classifications by the model were correct, while recall looks at how many of the existing positive data points were correctly classified [92]. Another metric, known as the F1 score, takes both of these factors into account; the F1 score is the harmonic mean of the precision and recall [91]. In our analysis, and because less than 13.5% of the original data points consisted of high-concentration events, we used recall as the primary metric.

3. Results and discussion

In this section, we first discuss the results of the down-selection of input signals, then the time series predictions and finally the results of the prediction of high-concentration events.

3.1. Determining best input combinations

We first present results of the down-selection process that evaluated the many combinations of possible inputs (as discussed in Section 2.1.1). Table 4 shows how many times each input variable appeared in the top five input combinations across the four RTT values and five repetitions of the model. For example, Table 4 shows that for CO_2 prediciton, the inputs "Hour" and "current hour of CO_2" appeared in all of the top combinations of inputs, and for next hour PM_1 prediction, indoor O_3 appeared 59 times out of a maximum of 100. The five inputs with the most predictive value for each predicted concentration are shown in Table 4.

Table 4 shows a few interesting results. First, as would be expected from the physics of the problem, the most predictive input for each pollutant was the previous hour's concentration. While this result may seem trivial, it is important to state because it serves as a sanity check of our methods. Next, non-air quality inputs play a substantial role in the prediction of most of the pollutants. For example, time of day ("Hour") appears in the top five most predictive inputs for 6 out of 8 pollutants and in the top 2 for the other 2 pollutants, suggest a strong diurnal pattern in concentrations (as would be expected for O_3 and indoor CO_2). Temperature inside and outside also seems predictive, although this was highly correlated with diurnal changes in temperature, meaning that it may be a confounder for the time of day. The day of the week appears in

Table 4
Number of times (in parentheses) each input shows up in the best performing combination of inputs for each predicted variable (left column in bold).

Outputs	# inputs analyzed	1st best	2nd best	3rd best	4th best	5th best
CO_2_in	9	CO_2_in (100)	Hour (100)	T_in (96)	T_out (79)	Num_week (79)
NO_2_in	11	NO_2_in (100)	NO_2_out (96)	T_out (83)	RH_out (79)	O3_out (69)
O_3_in	12	O_3_in (100)	Hour (100)	T_in (96)	Num_week (62)	Num_year (54)
PM_1_in	15	PM_1_in (100)	T_in (100)	PM_1_out (100)	Hour (93)	Num_week (81)
$PM_{2.5}$_in	15	$PM_{2.5}$_out (100)	$PM_{2.5}$_out (100)	T_in (96)	Hour (91)	Num_week (83)
PM_{10}_in	11	PM_{10}_in (100)	T_in (100)	PM_{10}_out (100)	Hour (92)	Num_week (83)
CH_2O	8	CH_2O (100)	CO_2_in (83)	T_out (76)	Num_week (75)	RH_in (72)
TVOC	8	TVOC (100)	CO_2_in (85)	RH_in (59)	NO_2_in (55)	PM_{10}_in (48)

the 6/8 top five lists, suggesting correlation with the work week habits of occupants and nearby polluting activity – such as motorists. The most interesting result was that (with a few exceptions) no pollutant signal appeared to aid in the prediction of any other pollutant. This was not what we expected considering conventional wisdom that pollutant concentrations are correlated because they issue from the same or related sources (e.g. automobiles on nearby streets or occupants of the building). The two exceptions to this pattern were HCHO and TVOC which appear to be predictable from the other pollutant signals. However, the prediction of these two elements was very poor (as we discuss in Section 3.2); hence, this result may be illusory.

3.2. Predicting the time series of concentrations

This section discussed how the different machine learning algorithms performed, both in terms of correctness of prediction and how far ahead each method could reasonably predict. We first present the results predicted 1 h in advance. The MSE and Adjusted R^2 resulting from use of the best input combinations for each method can be seen in Table 5. Several observations can be made from Table 5:

- The first observation is that the more sophisticated machine learning methods performed much better than the baseline. For the rolling average method, the training MSE ranged between 0.005 and 0.05, while the testing MSEs ranged between 0.007 and 0.08. This is approximately 1.5 orders of magnitude greater than those of the machine learning methods. This observation is confirmed by the R^2 values, which are poor for the rolling average method but considerably better for the machine learning methods.
- Substantial overfitting can be observed with the RF and GB methods. This is indicated primarily through the Adjusted R^2 values, which are notably worse on the validation set than the training set. For NO_2, the RF method yielded a training Adjusted R^2 value of 98.27%, indicating almost total representation of the variance in the training

data, while the validation Adjusted R^2 value was just 76.60%. Similar trends can also be observed in the results from CO_2.
- In all cases, the LSTM method performed better than any other method we tested on the validation datasets. In some cases, CO_2 for example, the training MSE and Adjusted R^2 values were indeed better for the RF and GB methods, but the LSTM method had better validation MSEs and Adjusted R^2 values. This result is in line with previous work showing that LSTM has superior performance in predicting sequential data than other methods such as RF and GB [90]. Although RF and GB are less computationally expensive and do not require advanced computational elements such as a GPU, they are insufficiently accurate in predicting sequential data. As expected, LSTM did much better at extracting patterns from input feature spaces that spanned long sequences [87].
- Prediction of HCHO and TVOCs was quite poor. This is likely due to inaccuracy in the sensor hardware and perennial difficulties in accurately quantifying the concentrations of these gases with low-cost sensors, but no definitive explanation can be given at the time.

Tables for two and 3 h look-aheads can be found in Appendix C.

Fig. 3 shows a plot of real versus estimated data for NO_2, for the best combination of input variables, and using a 20% RTT. Similar plots are given for the other pollutants and other prediction models in Appendix C.

Fig. 4 displays a comparison of MSE values for predicting different times into the future (1–3 h ahead) for each method. In Fig. 4 we show two illustrative examples, the CO_2 and $PM_{2.5}$ predictions. The LSTM method consistently had the least error and the least overfitting, while overfitting increased dramatically after an hour using the RF and GB methods. The LSTM method predictions did not show radical decrease in performance after 3 h, but were significantly less accurate. Graphs for the other pollutants can be found in Appendix C; the majority of the pollutants look like $PM_{2.5}$, while a few are CO_2.

Table 5
Hour-ahead indoor pollutant prediction [Training Mean Squared errors] Training Adjusted R^2 {Testing Mean Squared errors} (Testing Adjusted R^2).

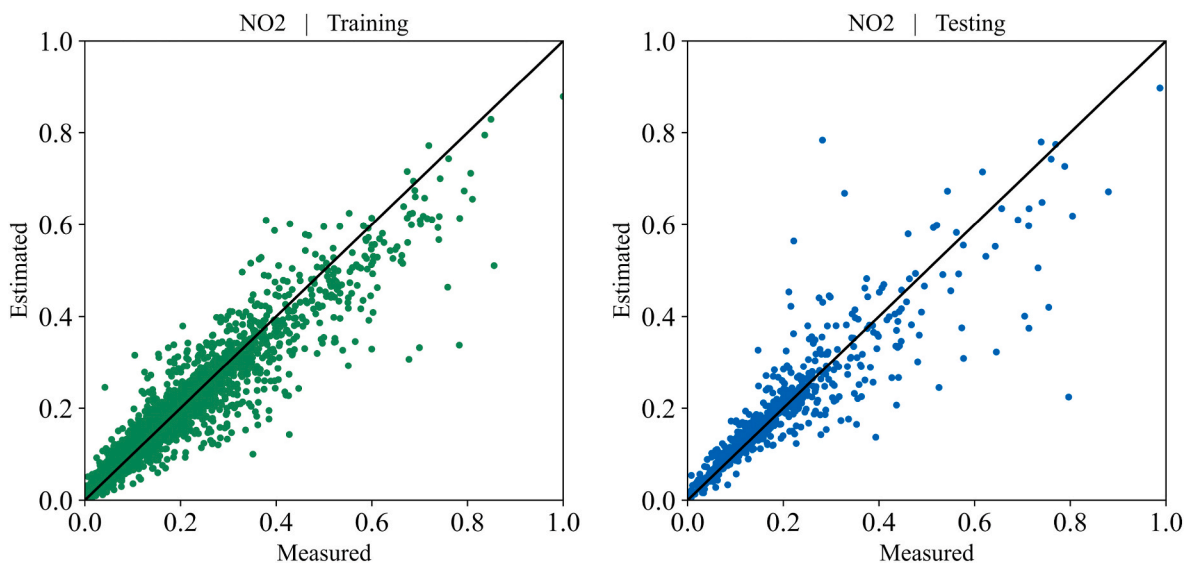| Method	CO_2	NO_2	O_3	PM_1	$PM_{2.5}$	PM_{10}	CH_2O	TVOC
Average	[0.045697]	[0.040134]	[0.028170]	[0.011167]	[0.012636]	[0.012184]	[0.010090]	[0.004979]
	−0.20%	25.40%	53.64%	75.98%	74.43%	73.55%	34.36%	29.27%
	{0.037571}	{0.048218}	{0.072395}	{0.008050}	{0.007295}	{0.007983}	{0.078506}	{0.011034}
	(−3.79%)	(23.34%)	(1.46%)	(58.14%)	(55.69%)	(50.04%)	(2.54%)	(35.20%)
Random	[0.000441]	[0.000316]	[0.000192]	[0.000248]	[0.000201]	[0.000217]	[0.000349]	[0.000398]
Forest	98.27%	98.27%	99.23%	99.31%	99.17%	99.13%	96.27%	95.90%
	{0.003197}	{0.004543}	{0.003554}	{0.001611}	{0.001096}	{0.001271}	{0.054821}	{0.019477}
	(83.55%)	(76.60%)	(88.82%)	(89.14%)	(88.12%)	(86.92%)	(23.93%)	(60.28%)
Gradient	[0.002277]	[0.001446]	[0.001172]	[0.001102]	[0.000787]	[0.000803]	[0.001467]	[0.001015]
Boosting	90.58%	91.71%	95.16%	96.90%	96.73%	99.13%	84.35%	89.56%
	{0.003235}	{0.004437}	{0.003119}	{0.001595}	{0.001083}	{0.001275}	{0.055129}	{0.019530}
	(83.42%)	(77.50%)	(90.03%)	(89.52%)	(88.31%)	(86.97%)	(23.51%)	(60.17%)
LSTM	**[0.002976]**	**[0.002195]**	**[0.001775]**	**[0.001803]**	**[0.001372]**	**[0.001520]**	**[0.002130]**	**[0.001996]**
	88.96%	**89.11%**	**94.14%**	**94.92%**	**93.99%**	**93.88%**	**77.64%**	**77.25%**
	{0.002893}	**{0.003410}**	**{0.002339}**	**{0.001170}**	**{0.000448}**	**{0.000919}**	**{0.056541}**	**{0.016909}**
	(82.49%)	**(82.29%)**	**(90.03%)**	**(86.39%)**	**(87.14%)**	**(86.28%)**	**(16.23%)**	**(62.09%)**

Fig. 3. Normalized real data against normalized estimated data for NO_2's best output.
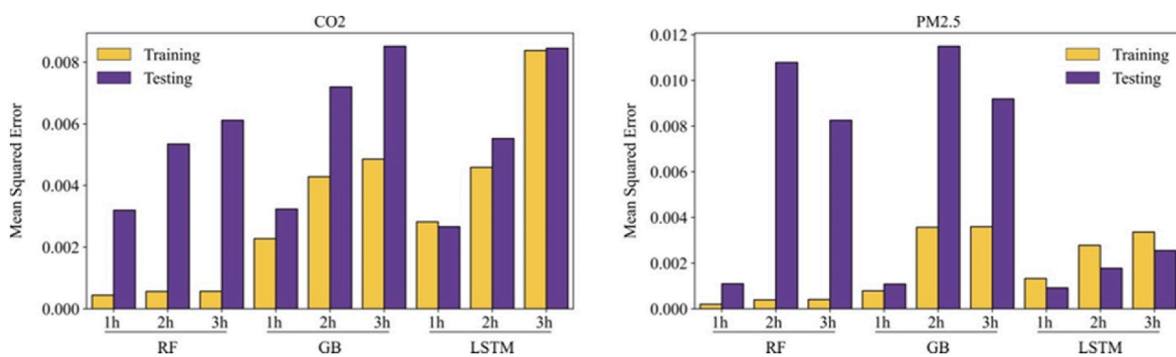

Fig. 4. Methods Comparison for CO_2 and $PM_{2.5}$ 1, 2, and 3 h ahead.

3.3. Event prediction

3.3.1. Using prediction models for classification

Table 6 presents the confusion matrix values, accuracy, precision, recall, and F1-score of the indirect event classification LSTM method for each indoor pollutant. Fig. 5 shows True Positive, True Negative, False Positive, and False Negative areas for NO_2 concentration after applying threshold (0.47). The sum of the true positive (TP) and false negative (FN) datapoints are equal to the number of high concentration events. We use Recall as the preferred measure of performance as Recall is effectively the fraction of the high concentration events that were accurately categorized.

3.3.2. Direct classification of events

Below in [Table 7] are the results of the second method we used to

predict high-concentration events: LSTM direct classification for each indoor pollutant. The header of the table indicates the pollutant that each column refers to. The true positive, false positive, true negative and false negative classification counts are reported, as well as the precision and recall. These values were calculated for the test set, which was the last 20% of the data with 600 total data points. Additionally, the accuracy and F1-scores are calculated and reported for each indoor pollutant. While the precision and recall of the model are less than ideal for all of the pollutants, the model is still capable of predicting upcoming events. Further optimization may yield better results.

3.3.3. Indirect and direct classification comparison

In Tables 6 and 7, the best results obtained for indirect and direct classification are compared. Using recall (considering true positive and false negative) as the primary metric, results show that direct

Table 6
Confusion matrix values for the best prediction model for the indoor pollutants.

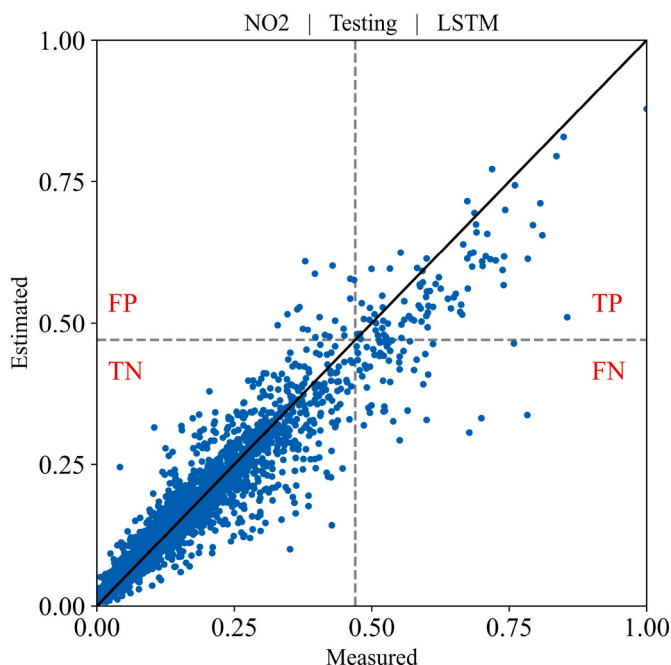|	CO_2	NO_2	O_3	PM_1	$PM_{2.5}$	PM_{10}	CH_2O	TVOC
True Positive	11	22	52	8	3	3	24	46
False Positive	5	9	7	3	2	1	15	9
True Negative	571	557	523	584	588	589	533	489
False Negative	13	12	18	5	7	7	28	56
Accuracy	97.00%	96.50%	95.83%	98.67%	98.50%	98.67%	92.83%	89.17%
Precision	68.75%	70.97%	88.14%	72.73%	60.00%	75.00%	61.54%	83.64%
Recall	45.83%	64.71%	74.29%	61.54%	30.00%	30.00%	46.15%	45.10%
F1 Score	55.00%	67.69%	80.62%	66.67%	40.00%	42.86%	52.75%	58.60%

Fig. 5. Real versus estimated data points in NO_2 concentration (The threshold of 0.47 shown as a horizontal dashed line corresponds to the mean of the dataset + two standard deviations, which we defined as the threshold for determining the classification of a high-concentration event as explained in Section 2.2.2).

classification prediction performed marginally better than indirect classification for all pollutants except O_3. However, if precision is used as the primary metric, indirect classification performs marginally better than direct classification. In essence, this shows that indirect classification has a tendency to underpredict event concentrations, thus leading to more false negatives than direct classification. Indirect classification is better at predicting normal concentrations because it has greater precision. Notably, indirect classification is better for predicting O_3, CH_2O, and TVOC high concentration events because the percentage of HCEs are greater than training (see Table 3). The reason, however, for this phenomenon is unknown.

4. Conclusions, limitations and future work

This work provides a case study, among the first of its kind, of the use of machine learning models to predict time series of indoor pollutant concentrations, and predict high concentration events. It also gives some information about the usefulness of one pollutant sensor signal for aiding in the prediction of another pollutant's concentration. The primary conclusions gathered from this study are (1) compared to a simple rolling average, machine learning methods decreased error in prediction by over an order of magnitude. The best performing ML models predicted around 90% of the variance in time series data for most pollutants, (2) LSTM was the most accurate predictive model of those we

tested. The GB and RF models were significantly overfitted to the training data. (3) As is understood by most researchers and reported in other works, the low-cost HCHO and TVOC sensors used in this work offered less useful information than sensors used to measure other airborne pollutants of concern in indoor environments. The predictions of those same sensor signals performed substantially worse than those for other pollutants, (4) this work did not show any evidence that sensing one pollutant to aid in prediction of a different pollutant added any improvement to the prediction. However, it appears that time of day and day of week aid considerably in prediction of indoor pollutant concentrations and should likely be included as inputs in any predictive algorithm for indoor pollutant concentrations, (5) while we tried two different methods for predicting when high-concentration events would occur, none were able to accurately classify more than 80% of high-concentration events (NO2 using direct classification). Other pollutant events were only predicted correctly 40% of the time, and (6)

Several limitations to this study exist. First, the models were built from five months of data covering the winter and spring seasons. While the nature of the use type of the building does not necessarily imply a large variation in occupancy patterns or other variables over the course of the year (such as in an academic building for example), there are likely to be different patterns in the air quality data in different seasons. This may mean that models developed in this work will be less applicable in other seasons. We are in the process of generating a much larger data set in many commercial buildings for establishing the robustness of these models more generally.

Another significant limitation of the current work is in the type of building in which the sensors were deployed. As stated, only a single commercial building (mostly office space) was used in this case study. Other types of buildings are likely to have different approaches that are more relevant. For example, Tang et al. (2020) [63] deployed similar sensors in residences and quite different results. The Random Forest method proved much more useful in residences than it did in the current work, and success in high-concentration event prediction was significantly greater than in the current work. There are many differences between this work and the work of Tang, including a factor of approximately 50 in the size of the datasets used and the fact that research grade instruments were used in Tang, and the Tang experiments were conducted in residences with presumably more regular patterns. This may explain to some degree why the LSTM method was more applicable in the current work, given the smaller amount of data.

In addition, in order that our work has near-term practical applicability, our focus with respect to sensors is to use low-cost, easily available sensors rather than specialized, more expensive sensors that may not be widely affordable. As different and higher-resolution types of sensors become affordable, appropriate machine learning models may differ from those in the current work.

Lastly, sensor signals were predicted based only on global data such as outdoor weather and time of day, and the time series of data from the single sensor suite in question. An improvement might be made by using a "network" approach where one sensor signal is predicted using inputs from multiple sensors distributed throughout the building, and also by including variables such as rates of change of sensor signals (as done in Tang et al.). Future work will explore these improvements. It should be

Table 7
Confusion matrix values for indoor pollutants in terms of classification LSTM method.

	CO_2	NO_2	O_3	PM_1	$PM_{2.5}$	PM_{10}	CH_2O	TVOC
True Positive	14	27	48	9	4	5	20	42
False Positive	12	15	7	8	14	25	26	15
True Negative	564	551	523	579	576	566	522	483
False Negative	10	7	22	4	6	4	32	60
Accuracy	96.33%	96.33%	95.17%	98.00%	96.67%	95.17%	90.33%	87.50%
Precision	53.85%	64.29%	87.27%	52.94%	22.22%	16.67%	43.48%	73.68%
Recall	58.33%	79.41%	68.57%	69.23%	40.00%	55.56%	38.46%	41.18%
F1 Score	56.00%	71.05%	76.80%	60.00%	28.57%	25.64%	40.82%	52.83%

noted that these datasets will be made publicly available to researchers when they are available.

We are also currently exploring the use of machine learning techniques that generate data – such as Generative Adversarial Networks (GANs) - along with more sophisticated techniques such as bi-directional LSTM that better preserve the spatiotemporal nature of the data as well as Gated Recurrent Units (GRU) that are more efficient with respect to computation. Early results from this approach appear to be promising, but significant additional work is needed. In addition, we are in the process of instrumenting our own built environment through a recently awarded grant so that we can build our own datasets over time. These datasets will be made publicly available to researchers when they are ready.

CRediT authorship contribution statement

Ahmad Mohammadshirazi: Writing – original draft, Software, Formal analysis, Data curation. **Vahid Ahmadi Kalkhorani:** Software, Visualization, Writing – original draft. **Joseph Humes:** Writing –

original draft, Software. **Benjamin Speno:** Software, Writing – original draft. **Juliette Rike:** Writing – original draft, Software. **Rajiv Ramnath:** Resources, Supervision, Formal analysis, Funding acquisition. **Jordan D. Clark:** Writing – review & editing, Supervision, Project administration, Funding acquisition, Conceptualization.

Declaration of competing interest

The authors declare that they have no known competing financial interests or personal relationships that could have appeared to influence the work reported in this paper.

Acknowledgments

Appendix A. Brief Summary of the More Popular Commercial Sensors

While an in-depth review of commercially available sensors is beyond the scope of this particular paper, we have added a brief summary of the more popular commercial sensors in to give the reader an overview of available products, their reported capabilities, and approximate cost.

Table A1
Survey of some available low-cost air quality sensors and studies investigating their performance in laboratories and indoor environments. Prices were current in 2021 and may be out of date.

Manufacturer	Models	Cost [$]	Measurements	Communication
Wicked Device	Air Quality Egg	180	Particles, RH,P,T, gases optional	D, E, W
HabitatMap	AirBeam2	249	Particles, RH, T	B,W, C
AirThinx	AirthinxIAQ	699	Particles, T, P, TVOC, CO2, RH, HCHO	B, W, C
IQAir	AirVisual Pro	269	Particles, CO2,T, RH	D,W
Awair	Element	149	Particles, T, RH, CO2, TVOC	W, B
	Omni		Particles, T, RH, CO2, TVOCs, Light, Noise	
CairPol	Cairclip	1130	Varies	C
Dylos	DC1100	240	Particles,	Serial:+40$
Foobot	Home	199	T, RH, TVOC	W
Purple Air	PA-II (PA-1)	249	Particles	Ser, W, SD + 30$
Shinyei	PMS1	1000	Particles	E
Speck		149	Particles, RH	USB, W
TSI	BlueSky	400	Particles, T, RH	Ser, SD

RH-Humidity; P-Barometric Pressure; T-Temperature; CO2-Carbon dioxide.
TVOCs-Total Volatile Organic Compounds; HCHO-Formaldehyde.
B-Bluetooth; C-Cellular; D-On board display; E-Ethernet; MSD-Micro SD; MUSB-Micro USB; W-Wifi; elec-simple electrical.

Appendix B. Results of interpolation for missing data

Results from interpolation of the missing data with four different methods, Rolling Average with seven data points, Random Forest, Gradient Boosting, and LSTM, are shown below. Cross validation was applied here to allow for better comparison of the methods. Rolling average was the least accurate method with MSEs for training ranging from 0.013 to 0.033. The rolling average method does not allow for a validation split, so no MSE for validation loss was calculated for this method.

With Random Forest, results on the training set exceeded that of all other methods, including LSTM. Training MSEs ranged between 0.001 and 0.006. However, results on the validation set indicated that the method didn't perform as well with the new data. Validation MSEs had higher values, ranging between 0.003 and 0.015. This indicates some degree of overfitting for this technique, as it performs excellently on the data it was trained on, with less useful results on other previously unseen data.

Gradient Boosting was less accurate than Random Forest with training MSEs between 0.004 and 0.015. The validation MSEs ranged between 0.006 and 0.02. LSTM had comparable results to Random Forest. Training MSEs from interpolating data using LSTM ranged between 0.001 and 0.007. Validation MSEs ranged from 0.001 to 0.003. This indicates that the LSTM methods did not experience overfitting as Random Forest did, while still retaining a high degree of accuracy, making it the method of choice. Table A1 displays all the training and validation MSEs obtained for CO_2, NO_2 and O_3.
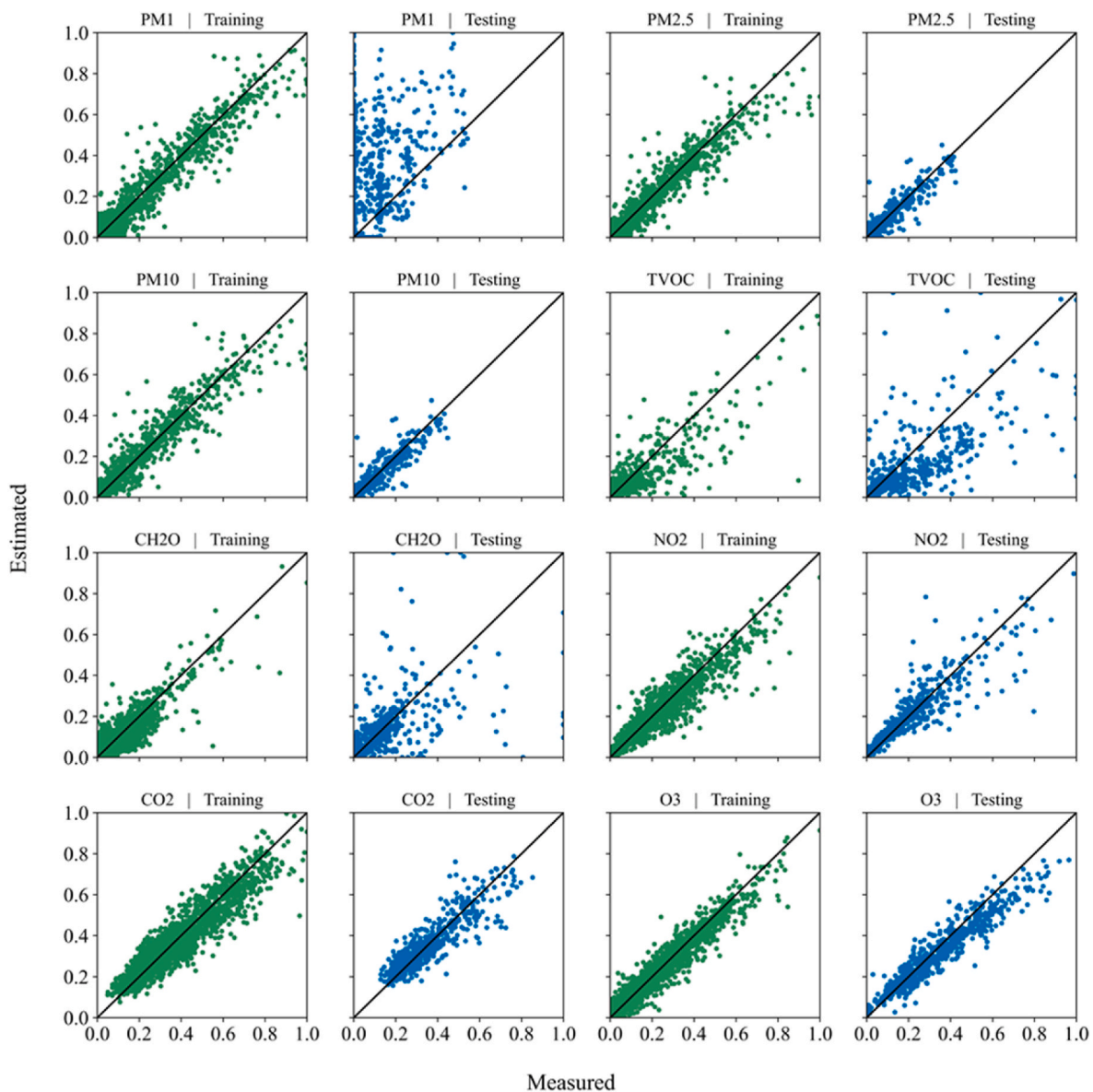
Table B1
Missing data results

Cross Validation Method	CO_2	NO_2	O_3
Average	[0.013625]	[0.021807]	[0.032612]
	{N/A}	{N/A}	{N/A}
Random Forest	[0.000575]	[0.00172]	[0.00137]
	{0.003734}	{0.012139}	{0.014704}
Gradient Boosting	[0.00453]	[0.00933]	[0.01511]
	{0.006918}	{0.011387}	{0.019305}
LSTM	**[0.0016]**	**[0.00611]**	**[0.00605]**
	{0.0014}	**{0.0023}**	**{0.0023}**

[Training Mean Squared errors].
{Cross Validation Mean Squared errors}.

Appendix C. Predicting time series concentrations

Figure C1 shows the results of the 1 h ahead predictions in graphical format, for both training and testing datasets, for each pollutant predicted.

Fig. C1. Normalized Real Data against Normalized Estimated Data for pollutants's Best Output

Tables C1 and C2 show results of the 2- and 3- hour ahead predictions in terms of Training MSEs (shown in []); Training Adjusted R^2 (shown without brackets); Testing MSEs (shown in {}); and Testing Adjusted R^2 (shown in ()). The evaluation metrics for the best performing methods are shown in bold, with LSTM being the best method in all cases for both 2-h and 3-h ahead predictions. Figure C2 shows the same information graphically.

Table C1
2 Hours-ahead indoor pollutant prediction

Method	CO_2	NO_2	O_3	PM_1	$PM_{2.5}$	PM_{10}
Average	[0.046128]	[0.046224]	[0.037694]	[0.015479]	[0.014615]	[0.014293]
	5.60%	21.78%	44.61%	70.22%	68.70%	67.39%
	{0.033901} (0.09%)	{0.039499} (22.33%)	{0.067006} (3.14%)	{0.004981} (31.40%)	{0.003951} (32.07%)	{0.005066} (27.16%)
Random Forest	[0.000563]	[0.000582]	[0.000270]	[0.000497]	[0.000393]	[0.000386]
	97.94%	97.03%	98.96%	98.66%	98.43%	98.52%
	{0.005347} (72.60%)	{0.006392} (71.57%)	{0.021489} (40.28%)	{0.015214} (6.31%)	{0.010788} (−10.87%)	{0.010981} (−4.78%)
Gradient Boosting	[0.004283]	[0.002898]	[0.003412]	[0.005119]	[0.003569]	[0.003774]
	84.33%	85.19%	86.80%	86.16%	85.76%	85.49%
	{0.007200} (63.11%)	{0.008710} (61.26%)	{0.019364} (46.19%)	{0.016865} (−3.85%)	{0.011498} (−18.16%)	{0.011279} (−7.63%)
LSTM	**[0.004589]**	**[0.003611]**	**[0.002901]**	**[0.004003]**	**[0.002779]**	**[0.002823]**
	83.33%	**81.71%**	**88.56%**	**89.18%**	**88.92%**	**89.15%**
	{0.005526} (71.45%)	**{0.007527} (65.84%)**	**{0.007539} (79.20%)**	**{0.002884} (81.41%)**	**{0.001777} (80.89%)**	**{ 0.002084} (79.14%)**

[Training Mean Squared errors].
Training Adjusted R.^{2}.
{Testing Mean Squared errors}.
(Testing Adjusted R^2).

Table C2
3 Hours-ahead indoor pollutant prediction

Method	CO_2	NO_2	O_3	PM_1	$PM_{2.5}$	PM_{10}
Average	[0.052349]	[0.050104]	[0.041299]	[0.055857]	[0.015946]	[0.015664]
	1.68%	15.77%	38.47%	5.94%	65.20%	63.83%
	{0.038298} (1.00%)	{0.042231} (16.80%)	{0.074096} (0.35%)	{0.039203} (0.34%)	{0.004304} (27.45%)	{0.005539} (22.44%)
Random Forest	[0.000567]	[0.000577]	[0.000276]	[0.000507]	[0.000408]	[0.000430]
	97.27%	97.05%	98.93%	98.62%	98.36%	98.34%
	{0.006118} (68.51%)	{0.007979} (64.41%)	{0.020530} (43.02%)	{0.015168} (6.64%)	{0.008258} (15.17%)	{0.008994} (14.22%)
Gradient Boosting	[0.004859]	[0.003859]	[0.003421]	[0.005089]	[0.003597]	[0.003869]
	82.23%	80.29%	86.75%	86.17%	85.58%	85.05%
	{0.008518} (56.15%)	{0.010475} (53.27%)	{0.019218} (46.67%)	{0.015808} (2.70%)	{0.009193} (5.57%)	{0.010855} (−3.54%)
LSTM	**[0.00838]**	**[0.008380]**	**[0.003791]**	**[0.005723]**	**[0.003358]**	**[0.003504]**
	69.55%	**69.55%**	**85.03%**	**84.54%**	**86.61%**	**86.54%**
	{0.008454} (56.33%)	**{0.008454} (56.33%)**	**{0.01057} (70.88%)**	**{0.004398} (71.68%)**	**{0.002552} (72.57%)**	**{ 0.002781} (72.18%)**

[Training Mean Squared errors].
Training Adjusted R.^{2}.
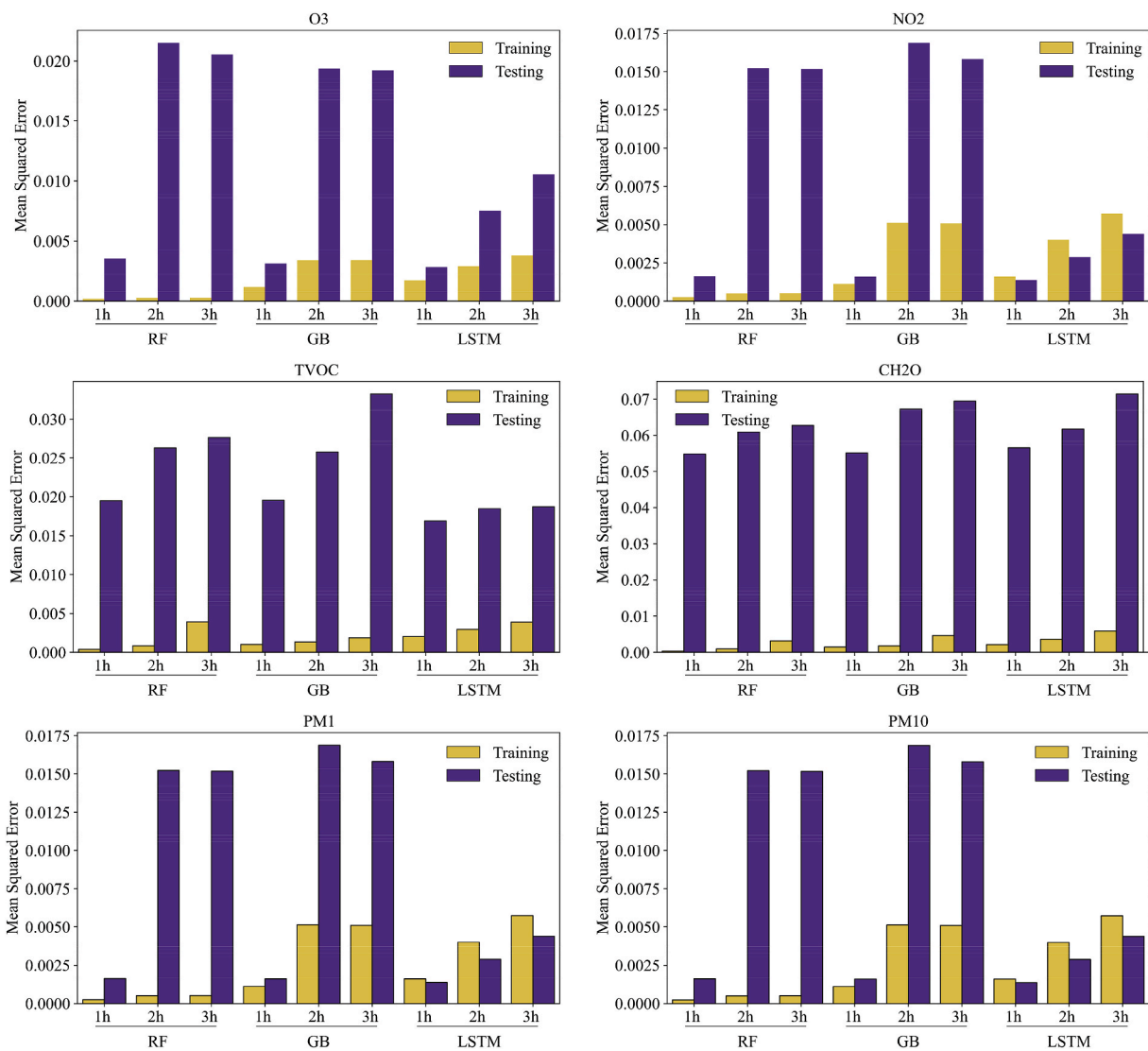{Testing Mean Squared errors}.
(Testing Adjusted R^2).

Fig. C2. Methods comparison for 1, 2, and 3 h ahead for O$_3$, NO$_2$, PM$_1$, and PM$_{10}$

References

[1] Environmental Protection Agency, Indoor Air Quality (IAQ), 2014.

[2] M. Falih, Ventilation for Acceptable Indoor Air Quality, ASHRAE, Atlanta, GA, 2019.

[3] U.S. Department of Energy, Baseline energy calculator. https://scout.energy.gov/baseline-energy-calculator.html, 2021. (Accessed 16 July 2021).

[4] H. Hao, C.D. Corbin, K. Kalsi, R.G. Pratt, Transactive control of commercial buildings for demand response, IEEE Trans. Power Syst. 32 (2017) 774–783, https://doi.org/10.1109/TPWRS.2016.2559485.

[5] S. Kiliccote, M.A. Piette, Advanced Control Technologies and Strategies Linking Demand Response and Energy Efficiency, 2005. Pittsburgh, PA.

[6] M. Young, B.D. Less, S.M. Dutton, I.S. Walker, M.H. Sherman, J.D. Clark, Assessment of peak power demand reduction available via modulation of building ventilation systems, Energy Build. 214 (2020) 109867, https://doi.org/10.1016/j.enbuild.2020.109867.

[7] P.H. Shaikh, N.B.M. Nor, P. Nallagownden, I. Elamvazuthi, T. Ibrahim, A review on optimized control systems for building energy and comfort management of smart sustainable buildings, Renew. Sustain. Energy Rev. 34 (2014) 409–429, https://doi.org/10.1016/j.rser.2014.03.027.

[8] J. Al Dakheel, C. Del Pero, N. Aste, F. Leonforte, Smart buildings features and key performance indicators: a review, Sustain. Cities Soc. 61 (2020) 102328, https://doi.org/10.1016/j.scs.2020.102328.

[9] G. Guyot, M. Sherman, I. Walker, J.D. Clark, Residential Smart Ventilation: A Review, Lawrence Berkeley National Laboratory, 2017.

[10] G. Guyot, M.H. Sherman, I.S. Walker, Smart ventilation energy and indoor air quality performance in residential buildings: a review, Energy Build. 165 (2018) 416–430, https://doi.org/10.1016/j.enbuild.2017.12.051.

[11] B.D. Less, S.M. Dutton, I.S. Walker, M.H. Sherman, J.D. Clark, Energy savings with outdoor temperature-based smart ventilation control strategies in advanced California homes, Energy Build. 194 (2019) 317–327, https://doi.org/10.1016/j.enbuild.2019.04.028.

[12] J.D. Clark, B.D. Less, S.M. Dutton, I.S. Walker, M.H. Sherman, Efficacy of occupancy-based smart ventilation control strategies in energy-efficient homes in the United States, Build. Environ. 156 (2019) 253–267, https://doi.org/10.1016/j.buildenv.2019.03.002.

[13] B. Less, I. Walker, D. Lorenzetti, E. Mills, V. Rapp, S. Dutton, et al., Smart ventilation for advanced California homes. https://doi.org/10.2172/1635274, 2020.

[14] S. Abraham, X. Li, A cost-effective wireless sensor network system for indoor air quality monitoring applications, Procedia Comput. Sci. 34 (2014) 165–171, https://doi.org/10.1016/j.procs.2014.07.090.

[15] S. Abraham, X. Li, Design of A Low-Cost wireless indoor air quality sensor network system, Int. J. Wireless Inf. Network 23 (2016) 57–65, https://doi.org/10.1007/s10776-016-0299-y.

[16] A.S. Ali, Z. Zanzinger, D. Debose, B. Stephens, Open Source Building Science Sensors (OSBSS): a low-cost Arduino-based platform for long-term indoor environmental data collection, Build. Environ. 100 (2016) 114–126, https://doi.org/10.1016/j.buildenv.2016.02.010.

[17] A. Curto, D. Donaire-Gonzalez, J. Barrera-Gómez, J.D. Marshall, M. J. Nieuwenhuijsen, G.A. Wellenius, et al., Performance of low-cost monitors to

assess household air pollution, Environ. Res. 163 (2018) 53–63, https://doi.org/10.1016/j.envres.2018.01.024.

[18] P.J. Dacunto, K.-C. Cheng, V. Acevedo-Bolton, R.-T. Jiang, N.E. Klepeis, J. L. Repace, et al., Real-time particle monitor calibration factors and PM2.5 emission factors for multiple indoor sources, Environ. Sci. Process Impacts 15 (2013) 1511, https://doi.org/10.1039/c3em00209h.

[19] P.J. Dacunto, N.E. Klepeis, K.-C. Cheng, V. Acevedo-Bolton, R.-T. Jiang, J. L. Repace, et al., Determining PM $_{2.5}$ calibration curves for a low-cost particle monitor: common indoor residential aerosols, Environ. Sci. Process Impacts 17 (2015) 1959–1966, https://doi.org/10.1039/C5EM00365B.

[20] R. Jayaratne, X. Liu, K.-H. Ahn, A. Asumadu-Sakyi, G. Fisher, J. Gao, et al., Low-cost PM2.5 sensors: an assessment of their suitability for various applications, Aerosol Air Qual. Res. (2020), https://doi.org/10.4209/aaqr.2018.10.0390.

[21] D. Thomas, B. Mistry, S. Snow, M.C. Schraefel, Indoor air quality monitoring (IAQ): a low-cost alternative to CO$$_{2}$$ monitoring in comparison to an industry standard device, in: K. Arai, S. Kapoor, R. Bhatia (Eds.), Intell. Comput., 858, Springer International Publishing, Cham, 2019, pp. 1010–1027, https://doi.org/10.1007/978-3-030-01174-1_77.

[22] L. Spinelle, M. Gerboles, M.G. Villani, M. Aleixandre, F. Bonavitacola, Field calibration of a cluster of low-cost commercially available sensors for air quality monitoring. Part B: NO, CO and CO2, Sensor. Actuator. B Chem. 238 (2017) 706–715, https://doi.org/10.1016/j.snb.2016.07.036.

[23] Y. Wang, Y. Du, J. Wang, T. Li, Calibration of a low-cost PM2.5 monitor using a random forest model, Environ. Int. 133 (2019) 105161, https://doi.org/10.1016/j.envint.2019.105161.

[24] M.D. Taylor, in: I.R. Nourbakhsh (Ed.), A Low-Cost Particle Counter and Signal Processing Method for Indoor Air Pollution, València, Spain, 2015, pp. 337–348, https://doi.org/10.2495/AIR150291.

[25] B.C. Singer, W.W. Delp, Response of consumer and research grade indoor air quality monitors to residential sources of fine particles, Indoor Air 28 (2018) 624–639, https://doi.org/10.1111/ina.12463.

[26] S. Patel, J. Li, A. Pandey, S. Pervez, R.K. Chakrabarty, P. Biswas, Spatio-temporal measurement of indoor particulate matter concentrations using a wireless network of low-cost sensors in households using solid fuels, Environ. Res. 152 (2017) 59–65, https://doi.org/10.1016/j.envres.2016.10.001.

[27] P. Kumar, A.N. Skouloudis, M. Bell, M. Viana, M.C. Carotta, G. Biskos, et al., Real-time sensors for indoor air monitoring and challenges ahead in deploying them to urban buildings, Sci. Total Environ. 560–561 (2016) 150–159, https://doi.org/10.1016/j.scitotenv.2016.04.032.

[28] A. Moreno-Rangel, T. Sharpe, F. Musau, G. McGill, Field evaluation of a low-cost indoor air quality monitor to quantify exposure to pollutants in residential environments, J. Sens. Sens. Syst. 7 (2018) 373–388, https://doi.org/10.5194/jsss-7-373-2018.

[29] A. Tiele, S. Esfahani, J. Covington, Design and development of a low-cost, portable monitoring device for indoor environment quality, J. Sens. (2018) 1–14, https://doi.org/10.1155/2018/5353816, 2018.

[30] Y. Wang, M. Boulic, R. Phipps, C. Chitty, A. Moses, R. Weyers, et al., Integrating open-source technologies to build a school indoor air quality monitoring box (SKOMOBO), in: 2017 4th Asia-Pac. World Congr. Comput. Sci. Eng. APWC CSE, IEEE, Nadi, 2017, pp. 216–223, https://doi.org/10.1109/APWConCSE.2017.00046.

[31] Y. Wang, J. Jang-Jaccard, M. Boulic, R. Phipps, C. Chitty, R. Weyers, et al., Deployment issues for integrated open-source — based indoor air quality school Monitoring Box (SKOMOBO), in: 2018 IEEE Sens. Appl. Symp. SAS, IEEE, Seoul, 2018, pp. 1–4, https://doi.org/10.1109/SAS.2018.8336758.

[32] K. Weekly, D. Rim, L. Zhang, A.M. Bayen, W.W. Nazaroff, C.J. Spanos, Low-cost coarse airborne particulate matter sensing for indoor occupancy detection, in: 2013 IEEE Int. Conf. Autom. Sci. Eng. CASE, IEEE, Madison, WI, USA, 2013, pp. 32–37, https://doi.org/10.1109/CoASE.2013.6653970.

[33] R. Weyers, J. Jang-Jaccard, A. Moses, Y. Wang, M. Boulic, C. Chitty, et al., Low-cost indoor air quality (IAQ) platform for healthier classrooms in New Zealand: engineering issues, in: 2017 4th Asia-Pac. World Congr. Comput. Sci. Eng. APWC CSE, IEEE, Nadi, 2017, pp. 208–215, https://doi.org/10.1109/APWConCSE.2017.00045.

[34] Y. Zou, J.D. Clark, A.A. May, A systematic investigation on the effects of temperature and relative humidity on the performance of eight low-cost particle sensors and devices, J. Aerosol Sci. 152 (2021) 105715, https://doi.org/10.1016/j.jaerosci.2020.105715.

[35] Z. Idrees, L. Zheng, Low cost air pollution monitoring systems: a review of protocols and enabling technologies, J. Ind. Inf. Integr. 17 (2020) 100123, https://doi.org/10.1016/j.jii.2019.100123.

[36] E. Austin, I. Novosselov, E. Seto, M.G. Yost, Laboratory evaluation of the Shinyei PPD42NS low-cost particulate matter sensor, PLoS One 10 (2015), e0137789, https://doi.org/10.1371/journal.pone.0137789.

[37] L. Bai, L. Huang, Z. Wang, Q. Ying, J. Zheng, X. Shi, et al., Long-term field evaluation of low-cost particulate matter sensors in Nanjing, Aerosol Air Qual. Res. 20 (2020) 242–253, https://doi.org/10.4209/aaqr.2018.11.0424.

[38] I. Demanega, I. Mujan, B.C. Singer, A.S. Anđelković, F. Babich, D. Licina, Performance assessment of low-cost environmental monitors and single sensors under variable indoor air quality and thermal conditions, Build. Environ. 187 (2021) 107415, https://doi.org/10.1016/j.buildenv.2020.107415.

[39] A. Caron, N. Redon, F. Thevenet, B. Hanoune, P. Coddeville, Performances and limitations of electronic gas sensors to investigate an indoor air quality event, Build. Environ. 107 (2016) 19–28, https://doi.org/10.1016/j.buildenv.2016.07.006.

[40] S. Collingwood, J. Zmoos, L. Pahler, B. Wong, D. Sleeth, R. Handy, Investigating measurement variation of modified low-cost particle sensors, J. Aerosol Sci. 135 (2019) 21–32, https://doi.org/10.1016/j.jaerosci.2019.04.017.

[41] H. Hojaiji, H. Kalantarian, A.A.T. Bui, C.E. King, M. Sarrafzadeh, Temperature and humidity calibration of a low-cost wireless dust sensor for real-time monitoring, in: 2017 IEEE Sens. Appl. Symp. SAS, IEEE, Glassboro, NJ, USA, 2017, pp. 1–6, https://doi.org/10.1109/SAS.2017.7894056.

[42] S. Jones, T.R. Anthony, S. Sousan, R. Altmaier, J.H. Park, T.M. Peters, Evaluation of a low-cost aerosol sensor to assess dust concentrations in a swine building, Ann. Occup. Hyg. 60 (2016) 597–607, https://doi.org/10.1093/annhyg/mew009.

[43] Y. Zou, M. Young, J. Chen, J. Liu, A. May, J.D. Clark, Examining the functional range of commercially available low-cost airborne particle sensors and consequences for monitoring of indoor air quality in residences, Indoor Air 30 (2020) 213–234, https://doi.org/10.1111/ina.12621.

[44] Y. Zou, M. Young, M. Wickey, A. May, J.D. Clark, Response of eight low-cost particle sensors and consumer devices to typical indoor emission events in a real home (ASHRAE 1756-RP), Sci. Technol. Built. Environ. 26 (2020) 237–249, https://doi.org/10.1080/23744731.2019.1676094.

[45] Y. Zou, J.D. Clark, A.A. May, Laboratory evaluation of the effects of particle size and composition on the performance of integrated devices containing Plantower particle sensors, Aerosol. Sci. Technol. (2021) 1–14, https://doi.org/10.1080/02786826.2021.1905148.

[46] Y. Wang, J. Li, H. Jing, Q. Zhang, J. Jiang, P. Biswas, Laboratory evaluation and calibration of three low-cost particle sensors for particulate matter measurement, Aerosol. Sci. Technol. 49 (2015) 1063–1077, https://doi.org/10.1080/02786826.2015.1100710.

[47] Z. Wang, W.W. Delp, B.C. Singer, Performance of low-cost indoor air quality monitors for PM2.5 and PM10 from residential sources, Build. Environ. 171 (2020) 106654, https://doi.org/10.1016/j.buildenv.2020.106654.

[48] F. Karagulian, M. Barbiere, A. Kotsev, L. Spinelle, M. Gerboles, F. Lagler, et al., Review of the performance of low-cost sensors for air quality monitoring, Atmosphere 10 (2019) 506, https://doi.org/10.3390/atmos10090506.

[49] S. Manibusan, G. Mainelis, Performance of four consumer-grade Air pollution measurement devices in different residences, Aerosol Air Qual. Res. 20 (2020) 217–230, https://doi.org/10.4209/aaqr.2019.01.0045.

[50] A. Manikonda, N. Zíková, P.K. Hopke, A.R. Ferro, Laboratory assessment of low-cost PM monitors, J. Aerosol Sci. 102 (2016) 29–40, https://doi.org/10.1016/j.jaerosci.2016.08.010.

[51] S. Sousan, K. Koehler, L. Hallett, T.M. Peters, Evaluation of consumer monitors to measure particulate matter, J. Aerosol Sci. 107 (2017) 123–133, https://doi.org/10.1016/j.jaerosci.2017.02.013.

[52] M.L. Zamora, J. Rice, K. Koehler, One year evaluation of three low-cost PM2.5 monitors, Atmos. Environ. 235 (2020) 117615, https://doi.org/10.1016/j.atmosenv.2020.117615.

[53] N. Zikova, P.K. Hopke, A.R. Ferro, Evaluation of new low-cost particle monitors for PM2.5 concentrations measurements, J. Aerosol Sci. 105 (2017) 24–34, https://doi.org/10.1016/j.jaerosci.2016.11.010.

[54] S. Chen, K. Mihara, J. Wen, Time series prediction of CO2, TVOC and HCHO based on machine learning at different sampling points, Build. Environ. 146 (2018) 238–246, https://doi.org/10.1016/j.buildenv.2018.09.054.

[55] I. Gryech, Y. Ben-Aboud, B. Guermah, N. Sbihi, M. Ghogho, A. Kobbane, MoreAir: a low-cost urban air pollution monitoring system, Sensors 20 (2020) 998, https://doi.org/10.3390/s20040998.

[56] B. Maag, Z. Zhou, L. Thiele, A survey on sensor calibration in air pollution monitoring deployments, IEEE Internet Things J. 5 (2018) 4857–4870, https://doi.org/10.1109/JIOT.2018.2853660.

[57] J. Ahn, D. Shin, K. Kim, J. Yang, Indoor air quality analysis using deep learning with sensor data, Sensors 17 (2017) 2476, https://doi.org/10.3390/s17112476.

[58] R. Piedrahita, Y. Xiang, N. Masson, J. Ortega, A. Collier, Y. Jiang, K. Li, R.P. Dick, Q. Lv, M. Hannigan, L. Shang, The next generation of low-cost personal air quality sensors for quantitative exposure monitoring, Atmos. Meas. Tech. 7 (10) (2014 Oct 7) 3325–3336, https://doi.org/10.5194/amt-7-3325-2014.

[59] A. Baldelli, Evaluation of a low-cost multi-channel monitor for indoor air quality through a novel, low-cost, and reproducible platform, Measurement: Sensors 17 (2021 Oct 1) 100059, https://doi.org/10.1016/j.measen.2021.100059.

[60] J.M. Logue, P.N. Price, M.H. Sherman, B.C. Singer, A method to estimate the chronic health impact of air pollutants in US residences, Environ. Health Perspect. 120 (2) (2012 Feb) 216–222, https://doi.org/10.1289/ehp.1104035.

[61] W.R. Chan, Y.S. Kim, B.D. Less, B.C. Singer, I.S. Walker, Ventilation and Indoor Air Quality in New California Homes with Gas Appliances and Mechanical Ventilation, Lawrence Berkeley National Lab.(LBNL), Berkeley, CA (United States), 2019 Feb, https://doi.org/10.2172/1509678.

[62] R. Zhang, H. Wang, Y. Tan, M. Zhang, X. Zhang, K. Wang, et al., Using a machine learning approach to predict the emission characteristics of VOCs from furniture, Build. Environ. 196 (2021) 107786, https://doi.org/10.1016/j.buildenv.2021.107786.

[63] H. Tang, W.R. Chan, M.D. Sohn, Automating the interpretation of PM2. 5 time-resolved measurements using a data-driven approach, Indoor Air 31 (3) (2021 May), 860-71, https://orcid.org/0000-0003-0361-0085.

[64] Z. Wang, T. Hong, M.A. Piette, Building thermal load prediction through shallow machine learning and deep learning, Appl. Energy 263 (2020) 114683, https://doi.org/10.1016/j.apenergy.2020.114683.

[65] C. Robinson, B. Dilkina, J. Hubbs, W. Zhang, S. Guhathakurta, M.A. Brown, et al., Machine learning approaches for estimating commercial building energy

consumption, Appl. Energy 208 (2017) 889–904, https://doi.org/10.1016/j.apenergy.2017.09.060.

[66] S. Seyedzadeh, F.P. Rahimian, I. Glesk, M. Roper, Machine learning for estimation of building energy consumption and performance: a review, Vis. Eng. 6 (2018) 5, https://doi.org/10.1186/s40327-018-0064-7.

[67] B. Zakeri, A.K. Monsefi, B. Darafarin, Deep learning prediction of heat propagation on 2-D domain via numerical solution, in: The 7th International Conference on Contemporary Issues in Data Science, Springer, Cham, 2019 Mar 6, pp. 161–174, https://doi.org/10.1007/978-3-030-37309-2_13.

[68] A.K. Monsefi, B. Zakeri, S. Samsam, M. Khashehchi, Performing software test oracle based on deep neural network with fuzzy inference system, in: International Congress on High-Performance Computing and Big Data Analysis, Springer, Cham, 2019 Apr 23, pp. 406–417, https://doi.org/10.1007/978-3-030-33495-6_31.

[69] B. Zakeri, A.K. Monsefi, S. Samsam, B.K. Monsefi, Weakly supervised learning technique for solving partial differential equations; case study of 1-d reaction-diffusion equation, in: International Congress on High-Performance Computing and Big Data Analysis, Springer, Cham, 2019 Apr 23, pp. 367–377, https://doi.org/10.1007/978-3-030-33495-6_28.

[70] E. Badrestani, B. Bahrak, A. Elahi, A. Faramarzi, P. Golshanrad, A.K. Monsefi, H. Mahini, A. Zirak, Real-time Travel Time Estimation Using Matrix Factorization, 2019 Dec 1 arXiv preprint arXiv:1912.00455.

[71] A.K. Monsefi, R. Bakhtiyarzade, Solving the Reaction-Diffusion Equation Based on Analytical Methods and Deep Learning Algorithm; the Case Study of Sulfate Attack to Concrete, 2019 Dec 7 arXiv preprint arXiv:1912.05452.

[72] Ronald Cohen, Alex Turner, Jinsol Kim, Helen Fitzmaurice, Katherine Chan, Pietro Vannucci, et al. BEACO2N n.d. http://beacon.berkeley.edu/(accessed July 18, 2021).

[73] AirNow Tech. Archive of outdoor air quality data n.d. https://files.airnowtech.org/(accessed July 18, 2021).

[74] PurpleAir. Sensor data download tool n.d. https://www.purpleair.com/sensorlist?key=71XU48F19Q4YGD4F&show=22463 (accessed July 18, 2021).

[75] B.C. Singer, W.W. Delp, Response of consumer and research grade indoor air quality monitors to residential sources of fine particles, Indoor Air 28 (4) (2018 Jul) 624–639, https://doi.org/10.1111/ina.12463.

[76] Y. Zou, J. Clark, A. May, Laboratory evaluation of the effects of particle size and composition on the performance of integrated devices containing Plantower particle sensor, Aerosol. Sci. Technol. 55 (7) (2021) 848–858, https://doi.org/10.1080/02786826.2021.1905148.

[77] 15x15 filtered 0-5 ppm NO2 sensor in pinned package. Spec. Sens. 2017. https://www.spec-sensors.com/wp-content/uploads/2016/10/3SP_NO2_5F-P-Package-110-507.pdf.

[78] 15x15 O3 sensor 20 ppm pinned package 110-406. Spec. Sens. 2019. https://www.spec-sensors.com/wp-content/uploads/2020/03/3SP_O3_20-P-Package-110-406.pdf.

[79] Smart NDIR gas sensors - cranberry, Mulberry & Foxberry. ELichens n.d. https://www.elichens.com/gas-sensors (accessed July 18, 2021).

[80] PMS 7003-PM2.5-plantower technology. PlanTower n.d. http://plantower.com/en/content/?110.html (accessed July 18, 2021).

[81] ZE07-CH2O formaldehyde gas sensor module. Winsen n.d. https://www.winsen-sensor.com/sensors/ch2o-gas-sensor/ze07-ch2o.html (accessed July 18, 2021).

[82] AMS CCS8xx product family of VOC sensors. AMS n.d. https://ams.com/-/ams-ccs8xx-product-family-of-voc-sensors-enhances-end-user-experience-for-indoor-air-quality-monitoring (accessed July 18, 2021).

[83] E. Zivot, J. Wang, Rolling analysis of time series, in: Model. Financ. Time Ser.-Plus®, Springer New York, New York, NY, 2003, pp. 299–346, https://doi.org/10.1007/978-0-387-21763-5_9.

[84] A. Liaw, M. Wiener, Classification and Regression by RandomForest, 2/3, 2002.

[85] Y. Li, C. Zou, M. Berecibar, E. Nanini-Maury, J.C. Chan, P. Van den Bossche, J. Van Mierlo, N. Omar, Random forest regression for online capacity estimation of lithium-ion batteries, Appl. Energy 15 (2018) 197–210, https://doi.org/10.1016/j.apenergy.2018.09.182, 232.

[86] J.H. Friedman, Stochastic gradient boosting, Comput. Stat. Data Anal. 38 (2002) 367–378, https://doi.org/10.1016/S0167-9473(01)00065-2.

[87] J. Cai, K. Xu, Y. Zhu, F. Hu, L. Li, Prediction and analysis of net ecosystem carbon exchange based on gradient boosting regression and random forest, Appl. Energy 15 (2020) 262, https://doi.org/10.1016/j.apenergy.2020.114566, 114566.

[88] S. Siami-Namini, N. Tavakoli, A. Siami Namin, A comparison of ARIMA and LSTM in forecasting time series, in: 2018 17th IEEE Int. Conf. Mach. Learn. Appl, ICMLA, 2018, pp. 1394–1401, https://doi.org/10.1109/ICMLA.2018.00227.

[89] S. Hochreiter, J. Schmidhuber, Long short-term memory, Neural Comput. 9 (1997) 1735–1780, https://doi.org/10.1162/neco.1997.9.8.1735.

[90] S. Ghimire, R.C. Deo, N. Raj, J. Mi, Deep solar radiation forecasting with convolutional neural network and long short-term memory network algorithms, Appl. Energy 1 (2019) 113541, https://doi.org/10.1016/j.apenergy.2019.113541, 253.

[91] D. Chicco, G. Jurman, The advantages of the Matthews correlation coefficient (MCC) over F1 score and accuracy in binary classification evaluation, BMC Genom. 21 (2020) 6, https://doi.org/10.1186/s12864-019-6413-7.

[92] N. Tatbul, T.J. Lee, S. Zdonik, M. Alam, J. Gottschlich, Precision and Recall for Time Series, 2019. ArXiv180303639 Cs.

[93] C.F. Bohren, D.R. Huffman, Absorption and scattering of. Light by small. https://doi.org/10.1209/0295-5075/113/47002, 1983.

[94] B.C. Singer, W.W. Delp, Response of consumer and research grade indoor air quality monitors to residential sources of fine particles, Indoor Air 28 (4) (2018 Jul) 624–639, https://doi.org/10.1111/ina.12463.

[95] W. Jiao, G. Hagler, R. Williams, R. Sharpe, R. Brown, D. Garver, R. Judge, M. Caudill, J. Rickard, M. Davis, L. Weinstock, Community Air Sensor Network (CAIRSENSE) project: evaluation of low-cost sensor performance in a suburban environment in the southeastern United States, Atmos. Meas. Tech. 9 (11) (2016 Nov 1) 5281–5292, https://doi.org/10.5194/amt-9-5281-2016.

[96] F.M. Bulot, S.J. Johnston, P.J. Basford, N.H. Easton, M. Apetroaie-Cristea, G. L. Foster, A.K. Morris, S.J. Cox, M. Loxham, Long-term field comparison of multiple low-cost particulate matter sensors in an outdoor urban environment, Sci. Rep. 9 (1) (2019 May 16) 1–3, https://doi.org/10.1038/s41598-019-43716-3.

[97] F.M. Bulot, H.S. Russell, M. Rezaei, M.S. Johnson, S.J. Ossont, A.K. Morris, P. J. Basford, N.H. Easton, G.L. Foster, M. Loxham, S.J. Cox, Laboratory comparison of low-cost particulate matter sensors to measure transient events of pollution, Sensors 20 (8) (2020 Jan) 2219, https://doi.org/10.3390/s20082219.

[98] W.R. Chan, J.M. Logue, X. Wu, N.E. Klepeis, W.J. Fisk, F. Noris, B.C. Singer, Quantifying fine particle emission events from time-resolved measurements: method description and application to 18 California low-income apartments, Indoor Air 28 (1) (2018 Jan) 89–101, https://doi.org/10.1111/ina.12425.

[99] I. Han, E. Symanski, T.H. Stock, Feasibility of using low-cost portable particle monitors for measurement of fine and coarse particulate matter in urban ambient air, J. Air Waste Manag. Assoc. 67 (3) (2017 Mar 4) 330–340, https://doi.org/10.1080/10962247.2016.1241195.

[100] R.M. Harrison, C.A. Thornton, R.G. Lawrence, D. Mark, R.P. Kinnersley, J. G. Ayres, Personal exposure monitoring of particulate matter, nitrogen dioxide, and carbon monoxide, including susceptible groups, Occup. Environ. Med. 59 (10) (2002 Oct 1) 671–679, https://doi.org/10.1136/oem.59.10.671.

[101] S. Feinberg, R. Williams, G.S. Hagler, J. Rickard, R. Brown, D. Garver, G. Harshfield, P. Stauffer, E. Mattson, R. Judge, S. Garvey, Long-term evaluation of air sensor technology under ambient conditions in Denver, Colorado, Atmos. Meas. Tech. 11 (8) (2018 Aug 8) 4605–4615, https://doi.org/10.5194/amt-11-4605-2018.

[102] D.M. Holstius, A. Pillarisetti, K.R. Smith, E.J. Seto, Field calibrations of a low-cost aerosol sensor at a regulatory monitoring site in California, Atmos. Meas. Tech. 7 (4) (2014 Apr 30) 1121–1131, https://doi.org/10.5194/amt-7-1121-2014.

[105] A.L. Northcross, R.J. Edwards, M.A. Johnson, Z.M. Wang, K. Zhu, T. Allen, K. R. Smith, A low-cost particle counter as a realtime fine-particle mass monitor, Environ. Sci.: Process. Impacts 15 (2) (2013) 433–439, https://doi.org/10.1039/C2EM30568B.

[106] S. Steinle, S. Reis, C.E. Sabel, S. Semple, M.M. Twigg, C.F. Braban, S.R. Leeson, M. R. Heal, D. Harrison, C. Lin, H. Wu, Personal exposure monitoring of PM2. 5 in indoor and outdoor microenvironments, Sci. Total Environ. 508 (2015 Mar 1) 383–394, https://doi.org/10.1016/j.scitotenv.2014.12.003.

[109] L.R. Crilley, M. Shaw, R. Pound, L.J. Kramer, R. Price, S. Young, A.C. Lewis, F. D. Pope, Evaluation of a low-cost optical particle counter (Alphasense OPC-N2) for ambient air monitoring, Atmos. Meas. Tech. 11 (2) (2018 Feb 7) 709–720, https://doi.org/10.5194/amt-11-709-2018.

[111] B. Feenstra, V. Papapostolou, S. Hasheminassab, H. Zhang, B. Der Boghossian, D. Cocker, A. Polidori, Performance evaluation of twelve low-cost PM2. 5 sensors at an ambient air monitoring site, Atmos. Environ. 216 (2019 Nov 1) 116946, https://doi.org/10.1016/j.atmosenv.2019.116946.

[103] Various assessments of air QUality measurement methods and their policy support project Website. https://vaquums.eu/sensor-db/sensors/envea-cairclip-o3-no2 (accessed January 6, 2022).

[104] M. Brauer, How much, how long, what, and where: air pollution exposure assessment for epidemiologic studies of respiratory disease, Proc. Am. Thorac. Soc. 7 (2) (2010 May 1) 111–115, https://www.atsjournals.org/doi/full/10.1513/pats.200908-093RM.

[107] D. Polidori, A. Sanghvi, R.J. Seeley, K.D. Hall, How strongly does appetite counter weight loss? Quantification of the feedback control of human energy intake, Obesity 24 (11) (2016 Nov) 2289–2295, https://doi.org/10.1002/oby.21653.

[108] S.T. Han, H. Peng, Q. Sun, S. Venkatesh, K.S. Chung, S.C. Lau, Y. Zhou, V.A. Roy, An overview of the development of flexible sensors, Adv. Mater. 29 (33) (2017 Sep) 1700375, https://doi.org/10.1002/adma.201700375.

[110] R. Duvall, A. Clements, G. Hagler, A. Kamal, V. Kilaru, L. Goodman, S. Frederick, K.J. Barkjohn, I. VonWald, D. Greene, T. Dye, Performance Testing Protocols, Metrics, and Target Values for Fine Particulate Matter Air Sensors: Use in Ambient, Outdoor, Fixed Sites, Non-regulatory Supplemental and Informational Monitoring Applications, US EPA Office of Research and Development, 2021 Feb. https://cfpub.epa.gov/si/si_public_record_Report.cfm?dirEntryId=350785&Lab=CEMM.

[112] C. Guo, Z. Zhang, A.K.H. Lau, C.Q. Lin, Y.C. Chuang, J. Chan, W.K. Jiang, T. Tam, E.K. Yeoh, T.C. Chan, L.Y. Chang, X.Q. Lao, Effect of long-term exposure to fine particulate matter on lung function decline and risk of chronic obstructive pulmonary disease in Taiwan: a longitudinal, cohort study, Lancet Planet. Health 2 (3) (2018) e114–e125, https://doi.org/10.1016/S2542-5196(18)30028-7.

[113] A. Khlystov, C. Stanier, S.N. Pandis, An algorithm for combining electrical mobility and aerodynamic size distributions data when measuring ambient aerosol special issue of aerosol science and technology on findings from the fine particulate matter supersites program, Aerosol. Sci. Technol. 38 (S1) (2004 Dec 1) 229–238, https://doi.org/10.1080/02786820390229543.

[114] Carnegie Mellon University. https://www.cmu.edu/news/stories/archives/2016/march/air-monitors-in-libraries.html#:~:text=The%20CREATE%20Lab%20and%20Airviz,infrared%20sensor%20to%20detect%20pollutants. (accessed January 6, 2022).